

# Raman-induced temporal condensed matter physics in gas-filled photonic crystal fibers

Mohammed F. Saleh,<sup>1,2,\*</sup> Andrea Armaroli,<sup>2</sup> Truong X. Tran,<sup>2,3</sup>  
Andrea Marini,<sup>2</sup> Federico Belli,<sup>2</sup> Amir Abdolvand,<sup>2</sup> and Fabio  
Biancalana<sup>1,2</sup>

<sup>1</sup>*School of Engineering and Physical Sciences, Heriot-Watt University, EH14 4AS Edinburgh, UK*

<sup>2</sup>*Max Planck Institute for the Science of Light, Günther-Scharowsky str. 1, 91058 Erlangen, Germany*

<sup>3</sup>*Department of Physics, Le Quy Don University, Vietnam*

[\\*m.saleh@hw.ac.uk](mailto:m.saleh@hw.ac.uk)

**Abstract:** Raman effect in gases can generate an extremely long-living wave of coherence that can lead to the establishment of an almost perfect temporal periodic variation of the medium refractive index. We show theoretically and numerically that the equations, regulate the pulse propagation in hollow-core photonic crystal fibers filled by Raman-active gas, are exactly identical to a classical problem in quantum condensed matter physics – but with the role of space and time reversed – namely an electron in a periodic potential subject to a constant electric field. We are therefore able to infer the existence of Wannier-Stark ladders, Bloch oscillations, and Zener tunneling, phenomena that are normally associated with condensed matter physics, using purely optical means.

© 2015 Optical Society of America

**OCIS codes:** (190.4370) Nonlinear optics, fibers; (190.5650) Raman effect; (190.5530) Pulse propagation and temporal solitons.

---

## References and links

1. P. St.J. Russell, “Photonic crystal fibers,” *Science* **299**, 358–362 (2003).
2. P. St.J. Russell, “Photonic-crystal fibers,” *J. Light. Technol.* **24**, 4729–4749 (2006).
3. J. C. Travers, W. Chang, J. Nold, N. Y. Joly, and P. St.J. Russell, “Ultrafast nonlinear optics in gas-filled hollow-core photonic crystal fibers,” *J. Opt. Soc. Am. B* **28**, A11–A26 (2011).
4. P. St.J. Russell, P. Hölzer, W. Chang, A. Abdolvand, and J. C. Travers, “Hollow-core photonic crystal fibres for gas-based nonlinear optics,” *Nat. Photon.* **8**, 278–286 (2014).
5. F. Benabid, J. C. Knight, G. Antonopoulos, and P. St.J. Russell, “Stimulated raman scattering in hydrogen-filled hollow-core photonic crystal fiber,” *Science* **298**, 399–402 (2002).
6. O. H. Heckl, C. R. E. Baer, C. Kränkel, S. V. Marchese, F. Schapper, M. Holler, T. Südmeyer, J. S. Robinson, J. W. G. Tisch, F. Couny, P. Light, F. Benabid, and U. Keller, “High harmonic generation in a gas-filled hollow-core photonic crystal fiber,” *Appl. Phys. B* **97**, 369 (2009).
7. N. Y. Joly, J. Nold, W. Chang, P. Hölzer, A. Nazarkin, G. K. L. Wong, F. Biancalana, and P. St.J. Russell, “Bright spatially coherent wavelength-tunable deep-uv laser source in ar-filled photonic crystal fiber,” *Phys. Rev. Lett.* **106**, 203901 (2011).
8. W. Chang, A. Nazarkin, J. C. Travers, J. Nold, P. Hölzer, N. Y. Joly, and P. St.J. Russell, “Influence of ionization on ultrafast gas-based nonlinear fiber optics,” *Opt. Express* **19**, 21018–21027 (2011).

9. P. Hölzer, W. Chang, J. C. Travers, A. Nazarkin, J. Nold, N. Y. Joly, M. F. Saleh, F. Biancalana, and P. St.J. Russell, "Femtosecond nonlinear fiber optics in the ionization regime," *Phys. Rev. Lett.* **107**, 203901 (2011).
10. M. F. Saleh, W. Chang, P. Hölzer, A. Nazarkin, J. C. Travers, N. Y. Joly, P. St.J. Russell, and F. Biancalana, "Soliton self-frequency blue-shift in gas-filled hollow-core photonic crystal fibers," *Phys. Rev. Lett.* **107**, 203902 (2011).
11. W. Chang, P. Hölzer, J. C. Travers, and P. St.J. Russell, "Combined soliton pulse compression and plasma-related frequency upconversion in gas-filled photonic crystal fiber," *Opt. Lett.* **38**, 2984–2987 (2013).
12. M. F. Saleh, W. Chang, J. C. Travers, P. St.J. Russell, and F. Biancalana, "Plasma-induced asymmetric self-phase modulation and modulational instability in gas-filled hollow-core photonic crystal fibers," *Phys. Rev. Lett.* **109**, 113902 (2012).
13. M. F. Saleh, A. Marini, and F. Biancalana, "Shock-induced  $\mathcal{PT}$ -symmetric potentials in gas-filled photonic crystal fibers," *Phys. Rev. A* **89**, 023801 (2014).
14. F. Belli, A. Abdolvand, W. Chang, J. C. Travers, and P. St.J. Russell, "Vacuum-ultraviolet to infrared supercontinuum in hydrogen-filled photonic crystal fiber," *Optica* **2**, 292–300 (2015).
15. S. Yoshikawa and T. Imasaka, "A new approach for the generation of ultrashort optical pulses," *Opt. Comm.* **96**, 94–98 (1993).
16. A. E. Kaplan, "Subfemtosecond pulses in mode-locked  $2\pi$  solitons of the cascade stimulated raman scattering," *Phys. Rev. Lett.* **73**, 1243–1246 (1994).
17. H. Kawano, Y. Hirakawa, and T. Imasaka, "Generation of high-order rotational lines in hydrogen by four-wave raman mixing in the femtosecond regime," *IEEE. J. Quantum Electron.* **34**, 260–268 (1998).
18. A. Nazarkin, G. Korn, M. Wittmann, and T. Elsaesser, "Generation of multiple phase-locked stokes and anti-stokes components in an impulsively excited raman medium," *Phys. Rev. Lett.* **83**, 2560–2563 (1999).
19. V. P. Kalosha and J. Herrmann, "Phase relations, quasicontinuous spectra and subfemtosecond pulses in high-order stimulated raman scattering with short-pulse excitation," *Phys. Rev. Lett.* **85**, 1226–1229 (2000).
20. G. Korn, O. Dühr, and A. Nazarkin, "Observation of raman self-conversion of fs-pulse frequency due to impulsive excitation of molecular vibrations," *Phys. Rev. Lett.* **81**, 1215–1218 (1998).
21. K. Ihara, C. Eshima, S. Zaitso, S. Kamitomo, K. Shinzen, Y. Hirakawa, and T. Imasaka, "Molecular-optic modulator," *Appl. Phys. Lett.* **88**, 074101 (2006).
22. M. Wittmann, A. Nazarkin, and G. Korn, "fs-pulse synthesis using phase modulation by impulsively excited molecular vibrations," *Phys. Rev. Lett.* **84**, 5508–5511 (2000).
23. G. H. Wannier, "Wave functions and effective Hamiltonian for Bloch electrons in an electric field," *Phys. Rev.* **117**, 432 (1960).
24. F. Bloch, "Über die Quantenmechanik der Electronen in Kristallgittern," *Z. Phys.* **52**, 555 (1928).
25. C. Zener, "A theory of electrical breakdown of solid dielectrics," *R. Soc. Lond. A* **145**, 523 (1934).
26. T. Pertsch, P. Dannberg, W. Elflein, A. Bräuer, and F. Lederer, "Optical Bloch oscillations in temperature tuned waveguide arrays," *Phys. Rev. Lett.* **83**, 4752 (1999).
27. R. Morandotti, U. Peschel, J. S. Aitchison, H. S. Eisenberg, and Y. Silberberg, "Experimental observation of linear and nonlinear optical Bloch oscillations," *Phys. Rev. Lett.* **83**, 4756 (1999).
28. M. Ghulinyan, C. J. Oton, Z. Gaburro, L. Pavesi, C. Toninelli, and D. S. Wiersma, "Zener tunneling of light waves in an optical superlattice," *Phys. Rev. Lett.* **94**, 127401 (2005).
29. A. Regensburger, C. Bersch, M. A. Miri, G. Onishchukov, D. N. Christodoulides, and U. Peschel, "Parity-time synthetic photonic lattices," *Nature* **488**, 167–171 (2012).
30. V. S. Butylkin, A. E. Kaplan, Y. G. Khronopulo, and E. I. Yakubovich, *Resonant Nonlinear Interaction of Light with Matter* (Springer-Verlag, 1989), 1st ed.
31. P. Kinsler, "Optical pulse propagation with minimal approximations," *Phys. Rev. A* **81**, 013819 (2010).
32. F. Belli, A. Abdolvand, W. Chang, J. C. Travers, and P. St.J. Russell, "Vacuum UV to IR supercontinuum generation by impulsive Raman self-scattering in hydrogen-filled PCF," in *CLEO: 2014, OSA Technical Digest* (online) (Optical Society of America, 2014), p. paper FW1D.1.
33. G. P. Agrawal, *Nonlinear Fiber Optics* (Academic Press, 2007), 4th ed.
34. M. J. Weber, *CRC Handbook of Laser Science and Technology Supplement 2: Optical Materials* (CRC press, 1994), 1st ed.
35. V. Mizrahi and D. P. Shelton, "Nonlinear susceptibility of  $\text{h}_2$  and  $\text{d}_2$  accurately measured over a wide range of wavelengths," *Phys. Rev. A* **32**, 3454–3460 (1985).
36. W. K. Bischel and M. J. Dyer, "Temperature dependence of the raman linewidth and line shift for the  $q(1)$  and  $q(0)$  transitions in normal and para- $\text{H}_2$ ," *Phys. Rev. A* **33**, 3113–3123 (1986).
37. R. A. Bartels, S. Backus, M. Murnane, and H. Kapteyn, "Impulsive stimulated raman scattering excitation of molecular vibrations via nonlinear pulse shaping," *Chem. Phys. Lett.* **374**, 326–333 (2003).
38. L. Gagnon and P. A. Bélanger, "Soliton self-frequency shift versus Galilean-like symmetry," *Opt. Lett.* **15**, 466–468 (1990).
39. A. M. Bouchard and M. Luban, "Bloch oscillations and other dynamical phenomena of electrons in semiconductor superlattices," *Phys. Rev. B* **52**, 5105 (1995).
40. G. J. Iafrate, J. P. Reynolds, J. He, and J. B. Krieger, "Bloch electron dynamics in spatially homogeneous electric

## 1. Introduction

Hollow-core photonic crystal fibers (HC-PCFs) continue to demonstrate their enormous potential for developing novel photonic devices for different optical applications [1, 2]. HC-PCFs with Kagome-style cladding structure have granted unprecedented strong interactions between light and gaseous media over relatively-long propagation distances with low transmission losses and pressure-tunable dispersion in the visible region [3, 4]. Within approximately a decade of the invention of the HC-PCF, exceptional nonlinear phenomena and applications have been demonstrated and predicted in these kind of fibers such as Stokes generation with drastical reduction in the Raman threshold [5], high harmonic generation [6], efficient deep-ultraviolet radiation [7], ionization-induced soliton self-frequency blueshift [8–11], strong asymmetrical self-phase modulation, universal modulational instability [12], and built-in parity-time symmetry [13].

The Raman effect is one of the earliest and most fundamental effects in nonlinear optics. When a pulse propagates inside a nonlinear medium, it excites optical phonons, leading to a plethora of phenomena, such as the generation of Stokes and anti-Stokes sidebands for long input pulses, and to an intense redshift for short pulses. The Raman effect has been successfully used to enhance the bandwidth of the output spectra during the supercontinuum generation, a dramatic spectral broadening due to the interaction of optical solitons, typically observed in solid-core optical fibers, and very recently in gas-filled HC-PCFs [14].

Stimulated Raman scattering processes in gases are characterized by a very long molecular coherence relaxation (dephasing) time, of the order of hundreds of picoseconds or more [14], which should be compared to the short relaxation time of phonon oscillations in silica glass (approx. 32 fs). Within this long relaxation phase, the medium exhibits a highly non-instantaneous response to pulsed excitations. Nonlinear interactions between optical pulses and Raman-active gases have been suggested and exploited mainly in the synthesis of subfemtosecond pulses using different techniques [15–19]. In addition, continuous down-shift of the frequency of an ultrashort pulse [20], and optical modulation of a continuous wave laser have been demonstrated [21] due to these interactions. Recently, some of the current authors have used the interaction of an ultrashort pulse with a hydrogen-filled HC-PCF to generate a supercontinuum extending from near infrared (1200 nm) to vacuum ultraviolet (124 nm) [14]. In the impulsive excitation regime, when the temporal pulse width is shorter than the Raman oscillation period of the gas, a sinusoidal temporal modulation of the medium refractive index lagging a pump source has been observed experimentally [18, 20, 22]. This modulation can be detected via launching a delayed weak probe within the dephasing time.

In this paper, we analyze the propagation of two temporally separated pulses in HC-PCFs filled with Raman-active gases. By investigating the effect of the Raman polarization induced by a pump pulse in the impulsive excitation regime, we demonstrate a perfect analogy between the spatiotemporal dynamics of a delayed probe and several phenomena observed in condensed matter physics, such as the Wannier-Stark ladder [23], Bloch oscillations [24] and Zener tunneling [25]. Although these effects have been previously observed in optics using periodic complex microstructures [26–29], our system is distinguished by the natural occurrence of a temporal periodic crystal via Raman excitation.

## 2. Governing equations for Raman media

Let us consider the propagation of an ultrashort pulse in a HC-PCF filled with a Raman-active gas. The medium response is described by its total polarization, which is a sum of the linear,

Kerr, and Raman polarizations. Ionization-induced plasma generation is neglected, as we assume that the pulse intensity is smaller than the gas ionization threshold. Assuming that only one Raman mode is excited (either the vibrational or rotational one), the dynamics of the Raman polarization (also called *coherence*)  $P_R$  can be determined by solving the Bloch equations for a two-level system [19, 30],

$$\begin{aligned} \partial_t w + \frac{w+1}{T_1} &= \frac{i\alpha_{12}}{\hbar} (\rho_{12} - \rho_{12}^*) E^2, \\ \left[ \partial_t + \frac{1}{T_2} - i\omega_R \right] \rho_{12} &= \frac{i}{2\hbar} [\alpha_{12} w + (\alpha_{11} - \alpha_{22}) \rho_{12}] E^2, \end{aligned} \quad (1)$$

where  $w = \rho_{22} - \rho_{11}$  is the population inversion between the excited and ground states,  $t$  is the time variable,  $\alpha_{ij}$  and  $\rho_{ij}$  are the elements of the  $2 \times 2$  polarizability and density matrices, respectively,  $E$  is the real electric field,  $\omega_R$  is the Raman frequency of the transition,  $N_0$  is the molecular number density,  $T_1$  and  $T_2$  are the population and polarization relaxation times, respectively, and  $\hbar$  is the reduced Planck's constant. Finally we have  $P_R \approx [\alpha_{12} (\rho_{12} + \rho_{12}^*) + \alpha_{11} \rho_{11} + \alpha_{22} \rho_{22}] N_0 E$ , assuming that initially all the molecules are in the ground state. In the regime where the slowly varying envelope approximation (SVEA) is valid, the electric field can be expressed as  $E = \frac{1}{2} [A(z, t) \exp(i\beta_0 z - i\omega_0 t) + c.c.]$ , where  $\omega_0$  is the pulse central frequency,  $\beta_0$  is the propagation constant calculated at  $\omega_0$ ,  $z$  is the longitudinal coordinate along the fiber,  $A$  is the complex envelope, and *c.c.* denotes the complex conjugate. We first introduce the following new variables:  $\xi = z/z_0$ ,  $\tau = t/t_0$ ,  $\psi = A/A_0$ ,  $z_0 = t_0^2 / |\beta_2(\omega_0)|$ ,  $A_0^2 = 1/(\gamma z_0)$ ,  $\gamma = 3\omega_0 \chi^{(3)} p_o T / (c^2 \epsilon_0 A_{\text{eff}} p T_o)$ , where  $\beta_2$  is the second-order dispersion coefficient,  $\gamma$  is the nonlinear Kerr coefficient in the unit of  $\text{W}^{-1} \text{m}^{-1}$ ,  $\chi^{(3)}$  is the third-order nonlinearity,  $p$  is the pressure,  $p_o$  is atmospheric pressure,  $T$  is the temperature,  $T_o = 273.15$  K,  $c$  is the speed of light,  $\epsilon_0$  is the vacuum permittivity,  $A_{\text{eff}}$  is the effective area of the fundamental mode, and  $t_0$  is the pulse duration. By using the SVEA, one can derive the following set of normalized coupled equations,

$$\begin{aligned} [i\partial_\xi + \hat{D}(i\partial_\tau) + |\psi|^2 + \eta \text{Re}(\rho_{12})] \psi &= 0, \\ \partial_\tau w + \frac{(w+1)t_0}{T_1} &= -4\mu w \text{Im}(\rho_{12}) |\psi|^2, \\ \left[ \partial_\tau + \frac{t_0}{T_2} - i\delta \right] \rho_{12} &= i\mu w |\psi|^2, \end{aligned} \quad (2)$$

where  $\hat{D}(i\partial_\tau) = z_0 \sum_{m \geq 1} \beta_m (i\partial_\tau)^m / t_0^m / m!$  is the full dispersion operator,  $\beta_m$  is the  $m$ th order dispersion coefficient calculated at  $\omega_0$ ,  $\eta = z_0/z_1$ ,  $z_1 = c\epsilon_0/(\alpha_{12} N_0 \omega_0)$  is the nonlinear Raman length,  $\mu = P_0/P_1$ ,  $P_0 = A_0^2$ ,  $P_1 = 2\hbar c \epsilon_0 A_{\text{eff}} / (\alpha_{12} t_0)$ ,  $\delta = \omega_R t_0$ , and  $\text{Re}$ ,  $\text{Im}$  represent the real and imaginary parts. In the derivation of Eq. (2), we have neglected the self-steepening effect, assumed that  $|w| \gg |\rho_{12}|$ , and the population inversion is weak, i.e.  $\rho_{11} \approx 1$ , and  $\rho_{22} \approx 0$ . These assumptions are physically realistic in gaseous Raman media under few- $\mu\text{J}$  input-pulse excitation. By comparing the outcomes of single pulse propagation in HC-PCFs filled by Raman-active gases, using our model and another full model based on the unidirectional pulse propagation equation that is not based on SVEA [14, 31], very good qualitative agreements, featured in obtaining the wiggled dispersive waves [32], between the two outputs have been obtained. It is worth also to note that the main condition  $\omega_0 t_0 \gg 1$  for the use of the SVEA [33] is satisfied in the simulations presented in this paper.

### 3. Raman response function

For femtosecond pulses, the relaxation times of the population inversion ( $T_1$ ) and the coherence ( $T_2$ ) can be safely neglected, since they are of the order of hundreds of picoseconds or more.

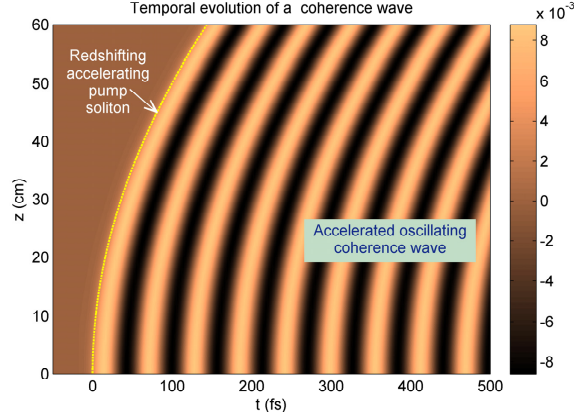


Fig. 1. Temporal evolution of an accelerated oscillating Raman polarization with period  $\Lambda = 56.7$  fs induced by a propagating fundamental soliton with an amplitude  $V_1 = 1.33$ , a central wavelength 1064 nm, and a FWHM 15 fs in a  $\text{H}_2$ -filled HC-PCF with a Kagome-lattice cross section, a flat-to-flat core diameter  $18 \mu\text{m}$ , a zero dispersion wavelength 413 nm, a gas pressure 7 bar, and a rotational Raman frequency  $\omega_R = 17.6$  THz. The dashed yellow line represents the temporal evolution of the soliton that excites the coherence wave. The simulation parameters are  $\gamma = 7.07 \times 10^{-6} \text{ W}^{-1} \text{ m}^{-1}$ ,  $\beta_2 = -3425.5 \text{ fs}^2/\text{m}$ ,  $A_{\text{eff}} = 134 \mu\text{m}^2$ ,  $\alpha_{12} = 0.8 \times 10^{-41} \text{ C m}^2/\text{V}$  [14, 34], and  $t_0 = 11.34$  fs. The parameter  $\gamma$  is calculated using the nonlinear susceptibility of  $\text{H}_2$  [35]. For these parameters, we have found that higher-order dispersion and self steepening effects have a weak influence on the soliton dynamics. All subsequent calculations in this paper are based on these values.

For instance,  $T_1 \approx 20$  ns and  $T_2 = 433$  ps for excited rotational Raman in hydrogen under gas pressure 7 bar at room temperature [14, 36]. This amazingly long relaxation times are a crucial and quite unique feature of gaseous Raman systems, which we use to the full in the present paper. We have also found that the population inversion is almost unchanged from its initial value for pulses with energies in the order of few  $\mu\text{J}$ , i.e.  $w(\tau) \approx w(-\infty) = -1$ . Hence, the set of the governing equations Eq. (2) can be reduced to a single generalized nonlinear Schrödinger equation,

$$i\partial_\xi \psi + i\frac{\beta_1 z_0}{t_0} \partial_\tau \psi + \frac{1}{2} \partial_\tau^2 \psi + |\psi|^2 \psi + R(\tau) \psi = 0, \quad (3)$$

where  $R(\tau) = \kappa \int_{-\infty}^{\tau} \sin[\delta(\tau - \tau')] |\psi(\tau')|^2 d\tau'$  is the resulting Raman convolution, and  $\kappa = \eta\mu$  is the ratio between the Raman and the Kerr nonlinearities. Pumping in the deep anomalous dispersion regime ( $\beta_2 < 0$ ) is assumed, hence, higher-order dispersion coefficients  $\beta_{m>2}$  can be neglected, so that the generation of dispersive waves is strongly reduced. For ultrashort pulses with duration  $t_0 \ll 1/\omega_R$ ,  $\sin[\delta(\tau - \tau')]$  can be expanded around the temporal location of the pulse peak by using a Taylor expansion. For instance, a fundamental soliton with amplitude  $V$  and centered at  $\tau = 0$  will induce a Raman contribution in the form of  $R(\tau) \approx \kappa V \sin(\delta\tau) [1 + \tanh(V\tau)]$  at the zeroth-order approximation. Hence, this soliton will generate a retarded sinusoidal Raman polarization that can impact the dynamics of the other trailing probe pulse lagging behind the pump pulse, see Fig. 1. On the other hand, for  $t_0 \gg 1/\omega_R$ ,  $R(\tau) \approx \gamma_R |\psi(\tau)|^2$  with  $\gamma_R = \kappa/\delta$ , i.e. the Raman nonlinearity is considered to be instantaneous. So, the Raman contribution would induce an effective Kerr nonlinearity that is significant, and can compete directly with the intrinsic Kerr nonlinearity of the gas [14, 37].



**Pump solution**— In the following, we will focus on two different pulses that are not overlapped in time, and separated by a delay  $\ll T_1, T_2$  in the deep anomalous dispersion regime. The leading pulse is an ultrashort strong ‘pump’ pulse  $\psi_1$  with  $t_0 \ll 1/\omega_R$ , while the trailing pulse is a weak ‘probe’ pulse  $\psi_2$  with negligible nonlinearity. In this case, Eq. (3) can be used to determine the pump solution. For weak Raman nonlinearity, the solution of Eq. (3) can be assumed to be a fundamental soliton that is perturbed by the Raman polarization, i.e.  $\psi_1(\xi, \tau) = V_1 \operatorname{sech}[V_1(\tau - u_1\xi - \bar{\tau}_1(\xi))]\exp[-i\Omega_1(\xi)(\tau - u_1\xi)]$  where  $u_1 = \beta_{11}z_0/t_0$ ,  $\beta_{11}$  is the first-order dispersion coefficient of the pump,  $V_1$ ,  $\Omega_1$ , and  $\bar{\tau}_1$  are the soliton amplitude, central frequency, and position of its peak, respectively. We will launch this soliton as a pump with  $\bar{\tau}_1(0) = 0$ . Using the variational perturbation method [33] and zeroth-order Taylor approximation, we have found that this soliton is linearly redshifting in the frequency domain with rate  $g_1 = \frac{1}{2}\kappa\pi\delta^2\operatorname{csch}(\pi\delta/2V_1)$ , and decelerating in the time domain, i.e.  $\Omega_1 = -g_1\xi$ , and  $\bar{\tau}_1 = g_1\xi^2/2$ . In the case  $t_0 < 1/\omega_R$ , we have found that a factor of  $\approx \frac{1}{2}$  might be used to correct the overestimated value of  $g_1$ , resulting from using the zeroth-order approximation.

#### 4. Governing equation for the probe

When a second weak probe pulse is sent after the leading pump soliton described in the previous section, the probe evolution is ruled by the equation

$$i\partial_\xi\psi_2 + iu_2\partial_\tau\psi_2 + \frac{1}{2m}\partial_\tau^2\psi_2 + 2\kappa V_1 \sin(\delta\bar{\tau})\psi_2 = 0, \quad (4)$$

where  $u_2 = \beta_{12}z_0/t_0$ ,  $m = |\beta_{21}|/|\beta_{22}|$ ,  $\beta_{1j}$  and  $\beta_{2j}$  are the first and the second order dispersion coefficients of the  $j^{\text{th}}$  pulse with  $j = 1, 2$ . Going to the reference frame of the leading decelerating soliton,  $\bar{\tau} = \tau - u_1\xi - g_1\xi^2/2$ , and applying a generalized form of the Gagnon-Bélanger phase transformation [38]  $\psi_2(\xi, \bar{\tau}) = \phi(\xi, \bar{\tau})\exp\left[i\bar{\tau}(g_1\xi + u_1 - u_2) + i(g_1\xi + u_1 - u_2)^3/6g_1\right]$ , Eq. (4) becomes

$$i\partial_\xi\phi = -\frac{1}{2m}\partial_{\bar{\tau}}^2\phi + [-2\kappa V_1 \sin(\delta\bar{\tau}) + g_1\bar{\tau}]\phi. \quad (5)$$

This equation is the *exact analogue* of the time-dependent Schrödinger equation of an electron in a periodic crystal in the presence of an external electric field. In Eq. (5) time and space are swapped with respect to the condensed matter physics system, as usual in optics, and we deal with a spatial-dependent Schrödinger equation of a single particle ‘probe’ with mass  $m$  in a *temporal crystal* with a periodic potential  $U = -2\kappa V_1 \sin(\delta\bar{\tau})$  in the presence of a constant force  $-g_1$  in the positive-delay direction. The ‘artificial electric field’  $g_1$  is not independent from the depth of the periodic potential  $2\kappa V_1$ . The leading soliton excites a sinusoidal Raman oscillation that forms a periodic structure in the reference frame of the soliton. Due to soliton acceleration induced by the strong spectral redshift, a constant force is applied on this structure. Substituting  $\phi(\xi, \bar{\tau}) = f(\bar{\tau})\exp(iq\xi)$ , Eq. (5) becomes an eigenvalue problem with eigenvectors  $f$ , and eigenvalues  $-q$ . The modes of this equation are the Wannier functions [23] that can exhibit Bloch oscillations [24], intrawell oscillations [39], and Zener tunneling [25] due to the applied force. Note that here we cannot use the so-called Houston functions [40] for solving Eq. (5), since these functions are valid only for small external electric fields - which is not the case. Hence, we must therefore calculate numerically the full solution of Eq. (5).

**Wannier-Stark ladder**— As a practical example, let us consider the propagation of an ultrashort soliton with FWHM 15 fs in a H<sub>2</sub>-filled HC-PCF with a Kagome lattice. The validity of the SVEA is maintained along the fiber, since the soliton does not suffer pulse compression and

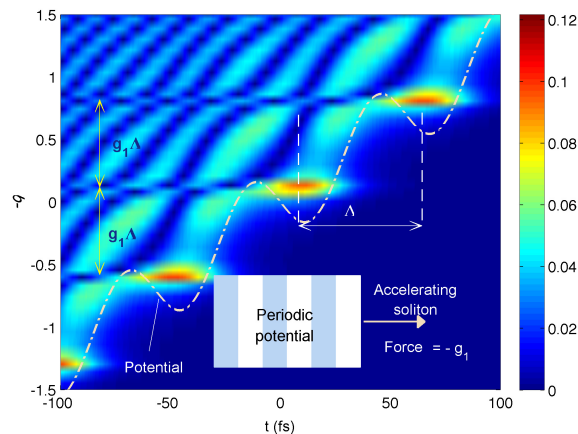


Fig. 2. A portion of the absolute eigenstates of a Raman-induced temporal periodic crystals with a lattice constant  $\Lambda = 56.7$  fs in the presence of a force with magnitude  $g_1 = 0.1408$  in the positive-delay direction. The vertical axis represents the corresponding eigenvalues  $-q$ . The dotted-dashed line is the potential under the applied force.

tends to preserve its shape during propagation. The assumptions of having weak higher-order dispersion coefficients and self-steepening effects have been checked. Also, the role of the vibrational Raman excitation with an oscillation 7 fs is modifying the Kerr nonlinearity. Exciting the rotational Raman shift frequency in the fiber via this soliton will induce a long-lived trailing *temporal periodic crystal* with a lattice constant  $\Lambda = 56.7$  fs, corresponding to the time required by the  $\text{H}_2$  molecule to complete one cycle of rotation, see Fig. 1. In the absence of the applied force, the solutions are the Bloch modes, while in the presence of the applied force, the periodic potential is tilted, and the eigenstates of the system are the Wannier functions portrayed as a 2D color plot in Fig. 2, where the horizontal axis is the time and the vertical axis is the corresponding eigenvalue. These functions are modified Airy beams that have strong or weak oscillating decaying tails. After an eigenvalue step  $g_1\Lambda$ , the eigenstates are repeated, but shifted by  $\Lambda$ , forming the Wannier-Stark ladder. As shown, each potential minimum can allow a single localized state with very weak tails. A large number of delocalized modes with long and strong tails exist between the localized states.

**Bloch oscillations and Zener tunneling—** An arbitrary weak probe following the soliton will be decomposed into the Wannier modes of the periodic temporal crystal. Due to beating between similar eigenstates in different potential wells, Bloch oscillations arise with a period  $\delta/g_1$ , while beating between different eigenstates in the same potential minimum can result in intrawell oscillations. In our case we did not observe in the simulations the latter kind of beating, since only a single eigenstate is allowed within each well. Interference between modes lying between different wells are responsible for Zener tunneling that allows transitions between different wells (or bands). In the absence of the applied force ( $g_1 = 0$ ), the band structure of the periodic medium can be constructed by plotting the propagation constants of the Bloch modes over the first Brillouin zone  $[-\delta/2, \delta/2]$ , as shown in Fig. 3(a). Zener tunneling occurs when a particle transits from the lowest band to the next-higher band. The evolution of a delayed probe in the form of the first Bloch mode inside a  $\text{H}_2$ -filled HC-PCF under the influence of the pump-induced temporal periodic crystal, is depicted in Fig. 3(b). Portions of the probe are localized in different temporal wells. Bloch oscillations are also shown with period 34.7 cm,

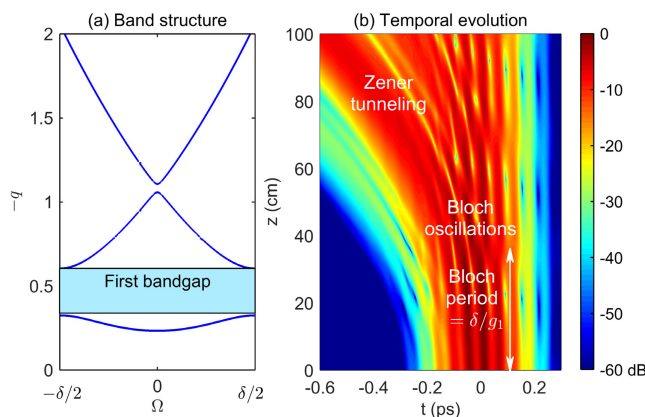


Fig. 3. (a) Bandstructure of the temporal crystal induced by the leading ultrashort soliton propagating in the H<sub>2</sub>-filled Kagome-lattice HC-PCF with  $m = 1$  in the absence of the applied force. (b) Temporal evolution of a weak probe in the accelerated periodic temporal crystal. The probe initial temporal profile is a Gaussian pulse with FWHM 133.6 fs superimposed on the first Bloch mode of the periodic crystal in the absence of the applied force. The contour plot is given in a logarithmic scale and truncated at -60 dB.

which correspond to the beating between localized modes in adjacent wells. After each half of this period, an accelerated radiation to the left due to Zener tunneling is also emitted. The Zener tunneling is dominant, and the Bloch oscillations are weak, because the potential wells are relatively far from each other. Hence, the overlapping between the localized modes are small, consistent with the shallowness of the first band in the periodic limit (absence of the applied force).

## 5. Conclusions

From the Maxwell-Bloch equations we have derived a model based on the slowly varying approximation that is convenient for investigating pulse propagation in HC-PCFs filled by Raman-active gases. We have specialized the model to study the propagation of two pulses that do not temporally overlap and are separated by a time delay smaller than the Raman polarization dephasing time ( $\sim 100$  ps). The leading pulse is an ultrashort strong soliton acting as a pump that experiences a linear redshift and deceleration due to Raman nonlinearity. Closed forms of the pump temporal and spectral dynamics have been obtained. The induced-Raman excitation creates a *temporal crystal* susceptible to a constant force due to the soliton acceleration. If the trailing pulse is assumed to be a weak probe, the problem is reduced to the motion of a particle in a periodic crystal subject to an external force. Phenomena such as Wannier-stark ladder, Bloch oscillations, and Zener tunneling have been demonstrated by simulations. Our results open new research pathways between nonlinear photonics and condensed-matter physics that will bear fruits not only for fundamental science but also for the conception of novel devices.

## Acknowledgments

The authors would like to acknowledge several useful discussions with Prof. Philip St.J. Russell and Dr. John Travers at Max Planck Institute for the Science of Light, Erlangen. The authors would like also to acknowledge the support of this research by the Royal Society of Edinburgh, Scottish Government, and German Max Planck Society for the Advancement of Science.